2011-8

Monofilar Spiral Slot Antenna for Dual-Frequency Dual-Sense Circular Polarization

Xiulong Bao
Technological University Dublin, xiulong.bao@tudublin.ie

Max Ammann
Technological University Dublin, max.ammann@tudublin.ie

Recommended Citation

Bao, X.L., & Ammann, M.J. (2011) Monofilar Spiral Slot Antenna for Dual-Frequency Dual-Sense Circular Polarization, *Transactions on Antennas & Propagation*, IEEE, vol. 59, no. 8, pp. 3061-3065, 08/2011. doi:10.1109/TAP.2011.2158964

Funder: Science Foundation Ireland

Monofilar Spiral Slot Antenna for Dual-Frequency Dual-Sense Circular Polarization

Xiulong Bao, Member, IEEE, Max J. Ammann, Senior Member, IEEE

Abstract— **A dual-band antenna with right-hand circular polarization for the first frequency and the counter polarization at the second frequency is realized with compact printed spiral slots. The coupled spiral slots are fed by a 50 Ω microstrip line. Dual-sense circularly-polarized performance is achieved by realizing oppositely-directed current rotation for the two frequency bands. A parametric study shows that the additional slot significantly improves the bandwidth for both frequency bands. Measured results show that the fractional impedance bandwidth is greater than 18% for both bands. The 3 dB axial-ratio bandwidths are 4.5% and 3.5% for the RHCP and LHCP bands, respectively.**

***Index Terms*— Dual Frequency, Dual Circular Polarization, Spiral Slot Antenna**

I. Introduction

CIRCULARLY-POLARIZED (CP) antennas have been used for decades for satellite communications and positioning systems and more recently for wireless communication and sensor system applications. This is due to advantages including immunity to Faraday rotation, mitigation of multipath propagation effects and reduced antenna orientation constraints. Many investigations have been carried out on broadbanding [1], miniaturization [2] and multiband operation of CP antennas [3]. Dual sense CP antennas have been also investigated [4], [5]. These antennas find application where dual-band reception of both RHCP and LHCP signals are required, such as in multimode GPS and Satellite Digital Audio Broadcast Systems. Other applications include wireless communications where dual CP offers improved isolation between channels compared to co-polarized systems.

It is well known that the spiral structure can achieve CP characteristics [6] and CP spiral slot antennas have been reported [7]. Double, triple and quadruple-arm spiral structures have realized wider CP bandwidths [8]-[10] and dual frequency spiral antennas [11] have been realized. Furthermore a single-arm spiral strip antenna has been reported which can achieve dual-sense CP by feeding either at the inner or outer spiral end [12].

In this paper, the first dual-frequency dual-sense CP performance from a spiral slot geometry is realized using a single microstrip feed. Furthermore, the introduction of an additional embedded spiral slot is shown to improve the axial-ratio (AR) bandwidth.

Manuscript received September 9, 2010. This publication has emanated from research conducted with the financial support of Science Foundation Ireland under Grant Number 09/SIRG/11644.

Xiulong. Bao and Max J. Ammann are with the Antenna and High Frequency Research Centre, Dublin Institute of Technology, Dublin 8, Ireland (email: ammann@ieee.org)

II. Configuration of the Proposed Spiral Slot Antennas

A. The Single Spiral Slot Antenna

The spiral slot antenna is initially investigated without the embedded slot for simplicity and can be seen in Fig. 1a-c. The slot is approximately one and a quarter turns long and the radius sequentially increases with movement of the origin point each quarter turn. The starting values are outer radius R_1 and origin O_1. The second quadrant has an outer radius R_2 and origin O_2. The 3rd, 4th and subsequent quadrants have radii R_3, R_4 and R_5 with origins O_3 O_4 and O_1, respectively. The slot maintains the same width W_1. In order to improve matching for both bands, the microstrip feedline width is stepped using lengths L_{s1}, L_{s2} and widths W_{s1} and W_{s2} as shown in Fig. 1a. Magnetic currents are excited on the slot, travelling out from the microstrip feed in opposite directions, establishing dual CP characteristics. The slot perimeter length corresponds approximately to one and two guided wavelengths for the first and second operating frequencies, respectively.

B. The Dual Spiral Slot Antenna

Fig. 1d shows the dual spiral slot antenna geometry, which consists of the above described spiral antenna with an additional smaller embedded concentric spiral slot. The smaller slot has outer radius values r_i (i = [1, 5]) and origin points O_i, (i = 1, 2, 3, 4, 1). The separation between the inner and outer spiral slot is S_c. The slot width is W_2.

III. Design Procedure

A. Single Spiral Slot Antenna

Firstly, the groundplane size was chosen to be 100 mm × 100 mm which is approximately a half of a free space wavelength at the lowest operating frequency. The antenna matching is sensitive to this dimension and it was chosen for best matching for both bands. A low-cost substrate with ε_r = 3.5, tanδ = 0.0018 and 1.57 mm of thickness was chosen.

Secondly, the 50 Ω microstrip feedline (W_{s2} = 3.0 mm) is stepped to W_{s1} = 1 mm (95 Ω) for good matching to the higher impedance slot.

Thirdly, the slot radius is increased to generate the spiral geometry. The origin O_1 is positioned centrally in the board

and an origin offset of $O_1O_2 = O_3O_4 = 2$ mm is used.

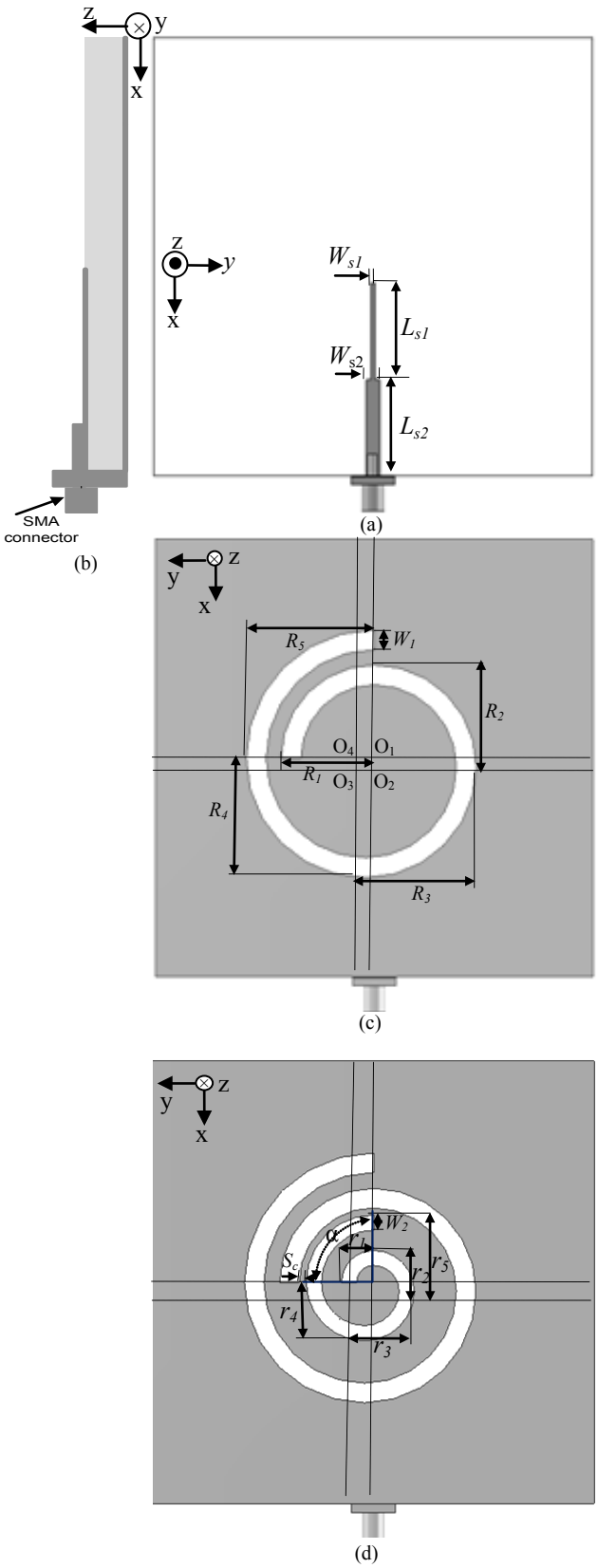

Fig. 1. Geometry of the proposed spiral slot antennas (a) Feedline (b) Profile (c) Single spiral slot antenna (d) Dual-slot spiral slot antenna

The starting slot radius R_1 is chosen to be approximately 1/8 of a guided wavelength λ_g for the lowest frequency. Subsequent radii increase by 2 mm per quarter-circle which was found to provide best axial-ratio (AR) and matching.

The operating frequencies, radiation patterns and AR beamwidth are dependent on the slot perimeter. The radiation patterns for a single-arm rectangular spiral antenna are dependent on the peripheral length of the spiral [13]. For peripheral lengths between λ_g and $2\lambda_g$, the radiation patterns are axial, whereas the pattern tilts off axis for lengths between $2\lambda_g$ and $3\lambda_g$.

In this case, the slot perimeter length approximates λ_g for the low frequency and a wide AR beamwidth is realized, whereas the slot length is about $2\lambda_g$ for the higher frequency and a narrow beamwidth is observed.

In order to investigate the mechanism for dual circular-polarization for the single spiral slot antenna, the current distribution for both low and high frequencies are shown in Fig. 2 (a) and (b).

It can be seen from Fig. 2 (a) that the resonant frequency for the low frequency (RHCP) is mainly determined by the outside length ($1/2 \times \pi \times (R_4+R_5)$), which is the circumference length from the feedpoint to the endpoint of the outside spiral slot and approximates a half of the guided wavelength. The full slot perimeter is about one guided wavelength at this frequency. As seen from Fig. 2 (b), the resonant frequency of the high frequency (LHCP) is mainly determined by the inner length ($1/2 \times \pi \times (R_1+R_2+R_3)$) which is the circumference length from the feedpoint to the endpoint of the inner spiral slot. This length in combination with some additional electrical lengthening due to coupling with the outside spiral approximates λ_g at the centre frequency for LHCP. The full slot perimeter is about $2\lambda_g$ at this frequency.

The low frequency current distribution shows the current traveling in an anti-clockwise fashion when viewed from the $+Z$ direction, leading to the radiation of a RHCP wave. The high frequency current travels in the opposite direction yielding a LHCP wave in the $+Z$ direction.

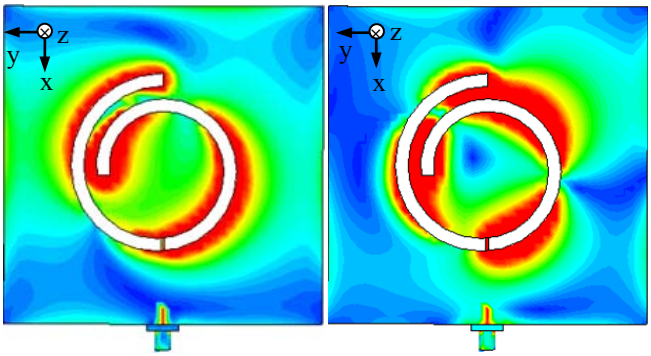

(a) low frequency (b) high frequency

Fig. 2. Surface current distributions for low and high bands

B. *Dual Spiral Slot Antenna*

Based on the investigation in this paper, dual-sense CP characteristics can be achieved by the single spiral slot antenna, but with very narrow AR bandwidth for the lower frequency band. Hence, the introduction of the second embedded spiral

slot is proposed to enhance matching and AR bandwidth for the low frequency band.

The smaller spiral slot is strongly coupled to the larger spiral slot for the first frequency band which significantly improves impedance matching and axial ratio. Furthermore, the smaller concentric spiral has little effect on the second band because of the relatively weak coupling at these frequencies. The slot perimeter length of the outer spiral slot is now approximately 1.17 λ_g at the lower frequency, whereas for the upper frequency, it remains at approximately $2\lambda_g$.

C. Comparison of S_{11} and Axial Ratio for the Single and Dual Spiral Slot Antennas

The parameters for the single and dual spiral slots are listed in Table 1.

Table 1 Parameters of the single and dual spiral slot antenna

Parameters	Single Spiral Antenna (mm)	Dual Spiral Antenna (mm)
R_1/r_1	21	21 / 7
R_2/r_2	23	23 / 9
R_3/r_3	25	25 / 11
R_4/R_4	27	27 / 13
R_5/R_5	29	29 / 15
L_{S1}	22	22
L_{S2}	22	22
W_{S1}	1	1
W_{S2}	3	3
W_1	4	4
W_2	-	3

The simulated S_{11} and AR are shown in Fig. 3 for the single and dual spiral antennas. The single spiral slot antenna exhibits narrow impedance bandwidth (S_{11}<-10 dB) and AR bandwidth (3 dB). The dual spiral exhibits significantly improved impedance bandwidth for the low band and wider AR bandwidths for both bands.

IV. PARAMETRIC STUDIES

The parametric study was made in order to evaluate the dual-band sensitivity to key parameters using the time domain solver in CST MWS. Other parameters were fixed as in Table 1.

a) Widths of the W_1 and slots W_2

The slot width plays a role in the antenna performance because it affects the input impedance. Fig. 4 shows the simulated S_{11} for various values of outer and inner slot widths W_1 and W_2. In this case, dual-frequency performance is optimum for slot widths of 3 mm or 4 mm. Fig. 5 shows that the low frequency shifts upwards as W_2 is varied from 2 mm to 3 mm. The frequency ratio f_2/f_1 can be tuned from 1.62 to 1.68.

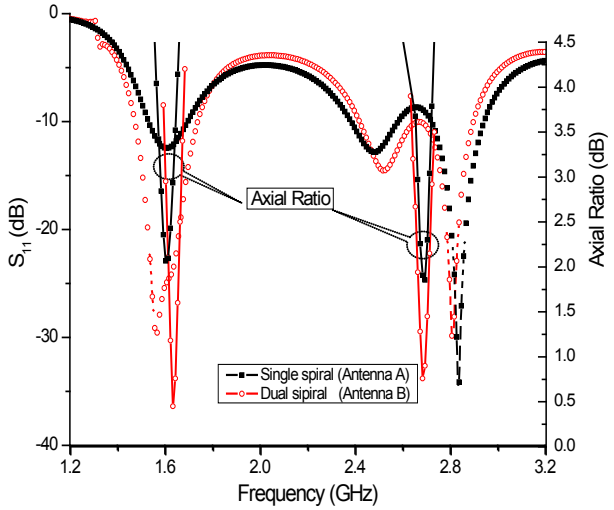

Fig. 3. Simulated S_{11} and AR for the single and dual spiral antennas

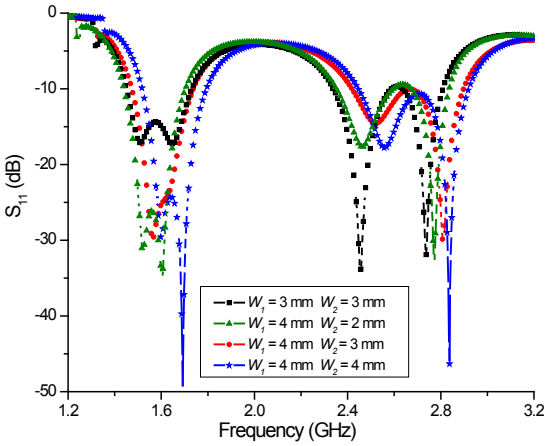

Fig. 4. Simulated S_{11} for various slot widths

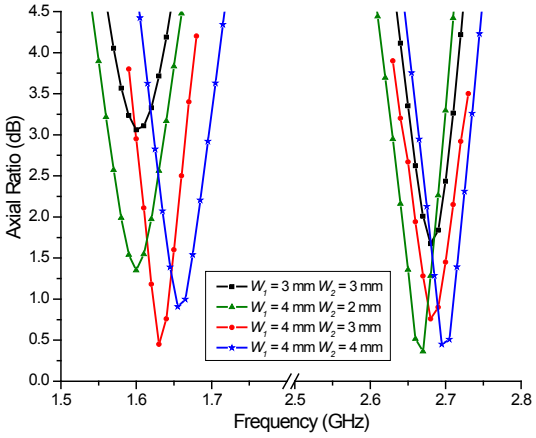

Fig. 5. Simulated axial ratio for various slot widths

b) Coupling between inside and outside spiral slots

The separation distance between inner and outer spirals slots can be used to control coupling and tailor the response of the antenna. Fig. 6 illustrates the simulated S_{11} for different values of coupling separation S_c. As the separation decreases, coupling is stronger with improved matching and an upward shift in

frequency for both bands. The low band frequency shifts upwards as the coupling distance S_c is varied from 1 mm to 3 mm. The frequency ratio of f_2 / f_1 can be tuned from 1.60 to 1.70 as shown in Fig. 7. The antenna is sensitive to the length over which the spirals couple, denoted here by a coupling angle α. Larger coupling angles improve matching for the low frequency whereas smaller angles improve the high frequency matching. The optimum angle for dual-band performance is α=90˚.

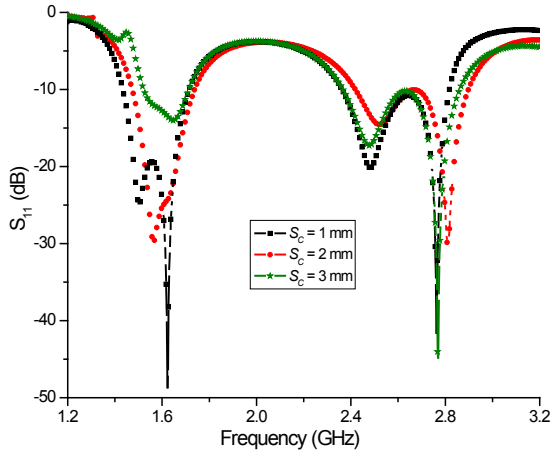

Fig. 6. Simulated S_{11} for various slot separation distances

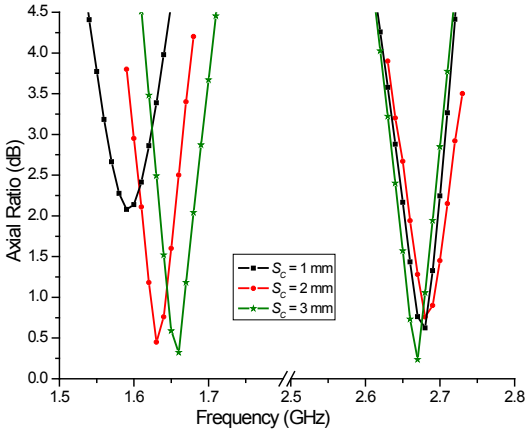

Fig. 7. Simulated axial ratio for various slot separation distances

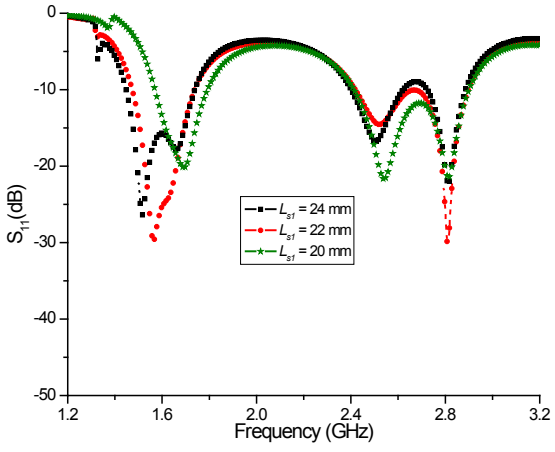

Fig. 8. Simulated S_{11} for various feedline lengths L_{SI}

c) The length of microstrip line L_{s1}

The simulated S_{11} for different values of microstrip feedline length Ls_1 is shown in Fig. 8. The low band shows greater sensitivity to this parameter and the impedance bandwidth decreases with decrease in line length. On other hand, the AR degrades as the length is increased as shown in Fig. 9. An appropriate feedline length is chosen to be 22 mm for best matching and AR bandwidth. For the dual spiral antenna, the microstrip feed couples to both inner and outer spiral slots. For shorter feedline lengths which couple only to the outer spiral, there is an upward shift in frequency and polarization becomes linear.

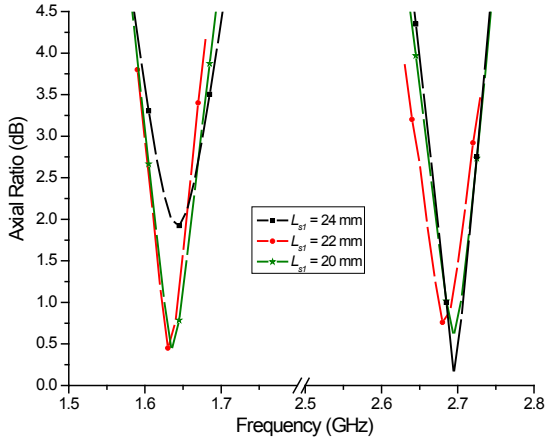

Fig. 9 Simulated axial ratio for various feedline lengths L_{SI}

V. Experimental Verification

The dual spiral slot antenna was fabricated on a Taconic RF35 laminate. Fig. 10 displays the measured and simulated S_{11} for the proposed antenna. The measurements show the impedance bandwidth to be 287 MHz (1.437 GHz to 1.724 GHz) or about 18.2% with respect to the centre frequency of 1.580 GHz for the first frequency band. For the second frequency band, the impedance bandwidth is 489 MHz (2.418 GHz to 2.907 GHz) or about 18.4% with respect to the centre frequency of 2.663 GHz.

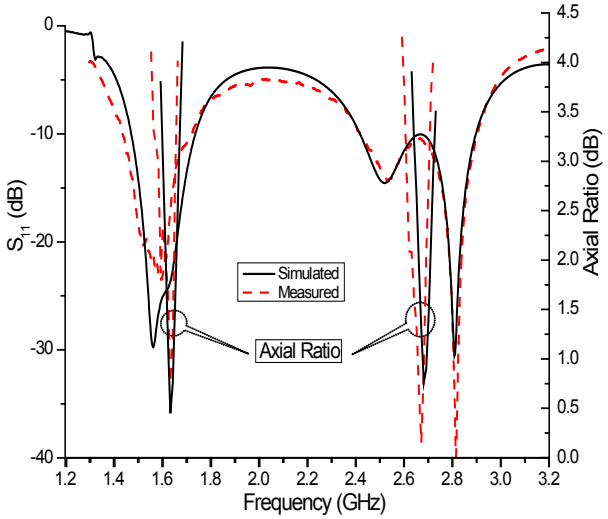

Fig 10. Measured and simulated S_{11} and axial ratio

Furthermore, Fig. 10 illustrates the measured and simulated AR plotted against frequency, which is also in good agreement. The measured result shows the 3 dB AR bandwidth to be 72 MHz (1.580 GHz to 1.652 GHz) or about 4.45% with respect to 1.616 GHz for the first band and 93 MHz (2.609 GHz to 2.702 GHz) or about 3.5% with respect to 2.655 GHz for the second band.

Fig. 11 and Fig. 12 show the measured and simulated normalized radiation patterns at 1.64 GHz and 2.68 GHz for the XoZ and YoZ planes, respectively. It is shown that the cross-polar levels are below 20 dB in the direction of the main beam.

There is good agreement between the measured results and simulated results. The RHCP radiation pattern at 1.64 GHz is symmetrical for the YoZ plane with a 3 dB beamwidth of 89° and offset by 10° for the XoZ plane with a beamwidth of 87°. For 2.68 GHz the LHCP pattern is symmetrical with a beamwidth of 57° for the YoZ plane and offset by 5° with beamwidth of 61° for the XoZ plane.

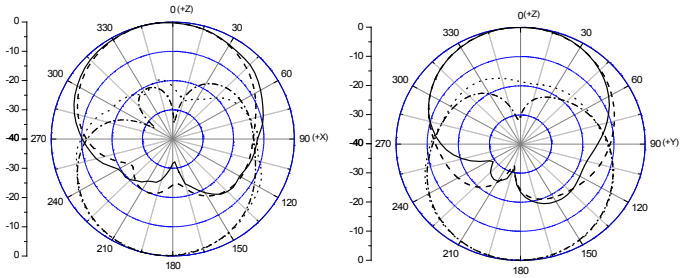

(a) (b)

Fig 11. The measured and simulated radiation patterns at 1.64 GHz (a) XoZ plane and (b) YoZ plane. Measured RHCP ——— Simulated RHCP - - - Measured LHCP ..... Simulated LHCP - . - .

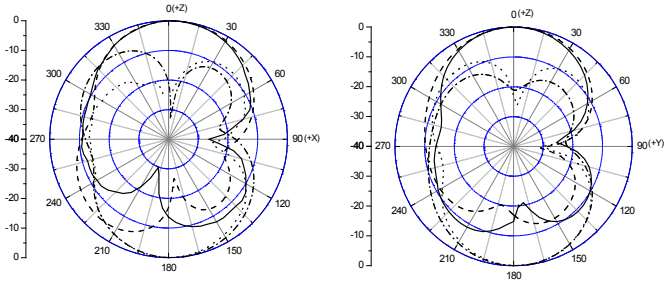

(a) (b)

Fig 12. The measured and simulated radiation patterns at 2.68 GHz (a) XoZ plane and (b) YoZ plane. Measured LHCP ——— Simulated LHCP - - - - Measured RHCP ..... Simulated RHCP - . - .

The measured gain values within the 3 dB AR bandwidths are from 3.9 dBic to 4.4 dBic for the low band and from 2.8 dBic to 3.8 dBic for the high band.

VI. Conclusion

A novel dual circularly-polarized monofilar spiral slot antenna was modeled, fabricated and tested. The proposed antenna can achieve RHCP and LHCP for the low and high frequency bands, respectively. The antenna realizes an 18% impedance bandwidth for both bands and AR bandwidths of 4.5% and 3.5% with respect to the centre frequencies of 1616 MHz and 2655 MHz, respectively.

References

[1] H. W. Kwa, X. M. Qing, and Z. N. Chen, Broadband Single-Fed Single-Patch Circularly Polarized Antenna for UHF RFID Applications, *IEEE Antennas and Propagation Society International Symposium*, July 2008, pp.1-4.

[2] X. L. Bao, and M. J. Ammann, Compact Annular-Ring Embedded Circular Patch Antenna with a Cross-Slot Ground Plane for Circular Polarization, *Electronics Letters*, Vol. 42, No. 4, 2006, pp.192-193.

[3] F. Jou, J. W. Wu, and C. J. Wang, Novel Broadband Monopole Antennas With Dual-Band Circular Polarization, *IEEE Transactions on Antennas and Propagation*, Vol. 57, No. 4, 2009, pp.1027-1034.

[4] C. H. Chen, and E. K. N. Yung, Dual-Band Dual-Sense Circularly-Polarized CPW-Fed Slot Antenna With Two Spiral Slots Loaded, *IEEE Transactions on Antennas and Propagation*, Vol. 57, No. 6, 2009, pp. 1829-1833.

[5] X. L. Bao, M. J. Ammann, Dual-frequency Dual-sense Circularly-polarized Slot Antenna Fed by Microstrip Line, *IEEE Transactions on Antennas and Propagation*, 2008, Vol. 56, No.3, pp. 645-649.

[6] W. L. Curtis, Spiral Antennas, *IRE Transactions on Antennas and Propagation*, Vol. 8, May 1960, pp.298-306.

[7] C. J. Wang, and D. F. Hsu, A Frequency-Reduction Scheme for Spiral Slot Antenna, *IEEE Antennas and Wireless Propagation Letters*, Vol. 1, 2002, pp. 161- 164.

[8] R. T. Gloutak, and N. G. Alexopoulos, Two-Arm Eccentric Spiral Antenna, *IEEE Transactions on Antennas and Propagation*, Vol. 45, No. 4, 1997, pp.723-730.

[9] D. J. Muller, and K. Sarabandi, Design and Analysis of a 3-Arm Spiral Antenna, *IEEE Transactions on Antennas and Propagation*, Vol. 55, No. 2, 2007, pp.258-266.

[10] N. A. Stutzke, and D. S. Filipovic, Four-Arm 2nd- Mode Slot Spiral Antenna With Simple Single-Port Feed, *IEEE Antennas and Wireless Propagation Letters*, Vol. 4, 2005, pp. 213-216.

[11] J. M. Laheurte, Dual-Frequency Circularly Polarized Antennas Based on Stacked Monofilar Square Spirals, *IEEE Transactions on Antennas and Propagation*, Vol.51, No.3, 2003, pp.488-492.

[12] C. W. Jung, B. A. Cetiner, and F. De. Flaviis, A Single-Arm Circular Spiral Antenna with Inner/Outer Feed Circuitry for Changing Polarization and Beam Characteristics, *2003 IEEE Antennas and Propagation Society International Symposium*, pp.474-477.

[13] H. Nakano, J. Eto, Y. Okabe, and J. Yamauchi, Tilted- and Axial-Beam Formation by a Single-Arm Rectangular Spiral Antenna With Compact Dielectric Substrate and Conducting Plane, *IEEE Transactions on Antennas and Propagation,* Vol. 50, No. 1, 2002, pp.17-23.